

# Impact properties of high-nitrogen austenitic stainless steels

Zhizhong Yuan\*, Qixun Dai, Xiaonong Cheng, Kangmin Chen, Wenwei Xu

*School of Materials Science and Engineering, Jiangsu University, Zhenjiang, Jiangsu 212013, People's Republic of China*

Received 12 December 2006; received in revised form 9 April 2007; accepted 13 April 2007

## Abstract

The Charpy v notch (CVN) impact properties of two kinds of high-nitrogen austenitic stainless steels (HNASS), Fe–24Mn–13Cr–1Ni–0.44N and Fe–24Mn–18Cr–3Ni–0.62N, were investigated at different temperatures. Results show that with the increase of nitrogen concentration, the absorbed-in-fracture energy decreases rapidly; microstructures, such as peeled off layer and transgranular brittle fracture facet (TBFF) are the features of brittle fracture of HNASSs when impacted at  $-190^{\circ}\text{C}$ . The transformation of fracture microstructures of them with the descending temperatures was also proposed.

© 2007 Elsevier B.V. All rights reserved.

*Keywords:* Austenitic stainless steel; Nitrogen; Impact property; Mechanical property

## 1. Introduction

Technologies, such as superconducting, have greatly advanced the research of cryogenic structural materials. There are some important requirements about this category of materials: (1) high yield strength; (2) superior toughness property at low temperature; (3) antimagnetic; (4) stable austenitic microstructure. The main cryogenic structural material is austenitic stainless steels and it has received great attention [1–6]. The development of cryogenic material is from Cr–Ni to Cr–Mn series steels because the Cr–Mn series steels have better combined properties of strength and toughness and most of them are strengthened by nitrogen, which is cheap and most effective. It is well known that the strength of the steel is in direct proportion to nitrogen content. Moreover, nitrogen can stabilize austenite but, at the same time, decrease the cryogenic toughness [7,8]. The toughness of high-nitrogen austenitic stainless steels (HNASS) at cryogenic temperatures is of great importance for the application of this kind of structural materials. Therefore, effects of nitrogen on cryogenic toughness of austenitic stainless steels have been intensively studied. Austenitic stainless steels with about 0.2 wt.% nitrogen can occur ductile to brittle fracture transformation, which was also found in nitrogen alloyed AISI304 steel by Di Schino et al. [9]. Tobler and Meyn [10] and Tomota et al. [11] discovered transgranular cleavage-

like fracture facet in Cr–Mn–N austenitic stainless steels, which is a totally different fracture mechanism. But there are few reports on the impact experiments at cryogenic temperatures of HNASS of Cr–Mn–N series and nitrogen content higher than 0.4 wt.%. Experiments on the materials of Fe–Mn–Cr–N series austenitic stainless steels with various nitrogen concentrations and impacted at different temperatures are necessary to reveal the ductile to brittle transformation temperature (DBTT) and to build a mathematical model for engineering application. Therefore, in this article, we developed two kinds of HNASSs based on our previous research [12–14] and investigated their impact properties, fracture microstructures and mechanism. We found that the HNASS with nitrogen content as high as 0.62 wt.% becomes brittle at  $-100^{\circ}\text{C}$ , which means the nitrogen content should be carefully controlled to make an optimum combination of yield strength and impact toughness.

## 2. Experimental details

The materials tested in this experiment are Fe–24Mn–13Cr–1Ni–0.44N and Fe–24Mn–18Cr–3Ni–0.62N, which are specified as 1# and 2#, respectively. The chemical compositions of them are shown in Table 1. They were fabricated in vacuum furnace and then forged into sheets of 16 mm in thickness. A solution treatment ( $1000^{\circ}\text{C}$  for 1 h, water cooling) was followed, which resulted in the austenitic structure. CVN samples were manufactured according to GB2106-80 (PR China) and tested in JBGD-300 impact test

\* Corresponding author. Tel.: +86 571 8795 1667; fax: +86 571 8795 2322.  
E-mail address: mseyuan@sohu.com (Z.Z. Yuan).

Table 1  
Compositions of experimental materials (wt.%)

Materials	C	Mn	Cr	Ni	Si	N	Fe
1#	0.050	24.62	13.18	0.10	0.57	0.44	Balance
2#	0.051	24.22	18.03	3.23	0.61	0.62	Balance

machine at 15,  $-100$  and  $-190$  °C, respectively. At each temperature, there are three samples for each kind of HNASS and the absorbed-in-fracture energy- $A_{kv}$  is the arithmetical mean of three experimental values. Fracture microstructures were investigated by JX-840 scanning electron microscope (SEM). All figures were taken at the center of the fractures.

### 3. Results and discussion

#### 3.1. Absorbed-in-fracture energy- $A_{kv}$

Experimental values (e.v.) of  $A_{kv}$  at different temperatures are shown in Fig. 1. Moreover, based on the equations,

$$A_{KV} (J) = A_{KV}^{300} \exp \left\{ -B \left[ \frac{300 - T}{300} \right]^2 \right\}, \quad A_{KV}^{300} = f(\text{Me}),$$

$$B = f(\text{Me})$$

developed by Cheng et al. [8], calculated values (c.v.) are also specified in Fig. 1. Given all allowable errors, the equation is useful for engineering application and materials design with satisfactory results. The yield strength at room temperature of 1# is lower than that of 2#, which has been proved experimentally [7]. But from Fig. 1, we can see that the impact toughness of 1# is better than that of 2#. The  $A_{kv}$  results of 1# and 2# at  $-190$  °C are the same, 14 J, which agrees with the results of ref. [15]. But the  $A_{kv}$  values of 1# are much higher than those of 2# when experimental temperature is  $-100$  °C, which means that brittle fracture dominates the 2# material from  $-190$  to  $-100$  °C. It can be deduced that the ductile to brittle transformation temperature (DBTT) is lower than  $-100$  °C for 1# but for 2#, higher than  $-100$  °C. Both the 1# and 2# are of ductile fracture with  $A_{kv}$  of 301 and 246 J, respectively, when they are impacted at 15 °C. Hanninen et al. [3] argued that nitrogen has a larger impact coefficient on  $A_{kv}$  than

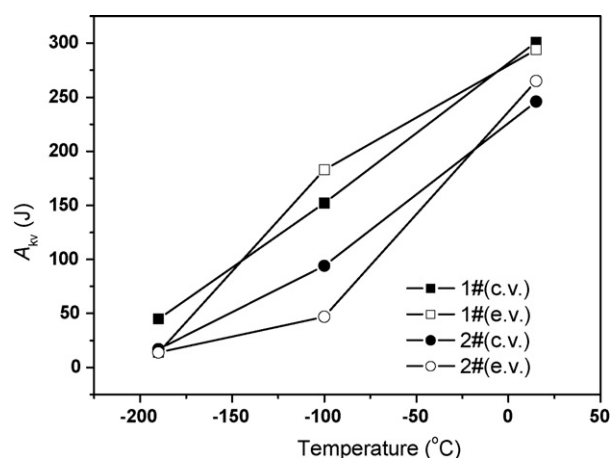


Fig. 1. The dependence of  $A_{kv}$  on temperature.

Mn, Ni and Cr, etc. And the impact toughness is very sensitive to nitrogen concentration. In this experiment, the test materials differ much in nitrogen content. Therefore, the difference of  $A_{kv}$  between 1# and 2# is mainly caused by the difference of nitrogen concentrations. Moreover, the nitrogen concentration should be carefully controlled to avoid brittle fracture at low temperature. Yoo et al. [16] found that low nitrogen content can improve the impact toughness of austenitic stainless steels. Dai and Huo [15] studied the impact toughness of Fe–28Mn–13Cr–0.5–1Mo with different nitrogen contents at low temperature and results show that there is an optimum impact toughness when nitrogen content is 0.32 wt.%. Therefore, it is not advisable to have too much nitrogen content. There must be a tradeoff between yield strength and impact toughness for the engineering application.

#### 3.2. Microstructures

Fractographs of both 1# and 2# impacted at different temperatures are shown in Fig. 2. Fig. 2a and b are fractures of 1# and 2# at 15 °C, respectively. They are both full of ductile cavities, which are typical microstructures of ductile fracture. But for 1#, most ductile cavities are stretched. While for 2#, most of them are equiaxial. For 1# and 2# impacted at  $-100$  °C, so called transgranular brittle fracture facets (TBFF) [15] appear but most of them are surrounded by ductile cavities (Fig. 2c and d, respectively). At  $-100$  °C, most of TBFFs are located at the bottom of the ductile cavities, which indicates that they are at the stage of transformation from ductile fracture to brittle fracture. We can also find that TBFF has larger percentage of area in 2# than in 1#, which means that 2# is more brittle than 1# and this result is consistent with the  $A_{kv}$  results. At  $-100$  °C, the difference of experimental  $A_{kv}$  between 1# and 2# is about 150 J. And for 2#, the low  $A_{kv}$  means it become brittle at this temperature. Fig. 2e and f are fractographs at  $-190$  °C of 1# and 2#, respectively, which are full of TBFFs. Both of them are brittle fractures.

Some special microstructure features are shown in Fig. 3. Quasi-equilateral triangle formed by crossed slip lines on fracture facet is shown in Fig. 3a, which are the characteristic of slip system on  $\{111\}_\gamma$  [16–18] and discovered in fractures of both 1# and 2# at temperatures lower than  $-100$  °C. In Fig. 3b, the parallel slip lines cross several slip planes, which is typical for TBFF of both 1# and 2#. Fig. 3c is twin crystal with slip lines in 2#, which is not seen in 1#. Twinning is one of the deformation modes other than slipping and seldom appears in austenitic structures unless the material has poor plasticity and under large stress concentration. Therefore, the twinning grains are common in 2# impacted at  $-190$  °C. Peeled off layers is shown in Fig. 3d, which can be found in both materials impacted at  $-190$  °C. If compared with those impacted at  $-100$  °C, fractographs at  $-190$  °C for both 1# and 2# are featured by TBFFs with larger area, peeled off layers, and closer spaced slip lines. The latter is caused by stress concentration, which is resulted from the synthetic effects of high nitrogen content and the low temperature. In a word, the transformation of fracture microstructures of both 1# and 2# with the decrease of temperature is illustrated in Fig. 4.

The peeled off layer has special reason for its formation and important meaning for HNASSs. Due to their high nitrogen con-

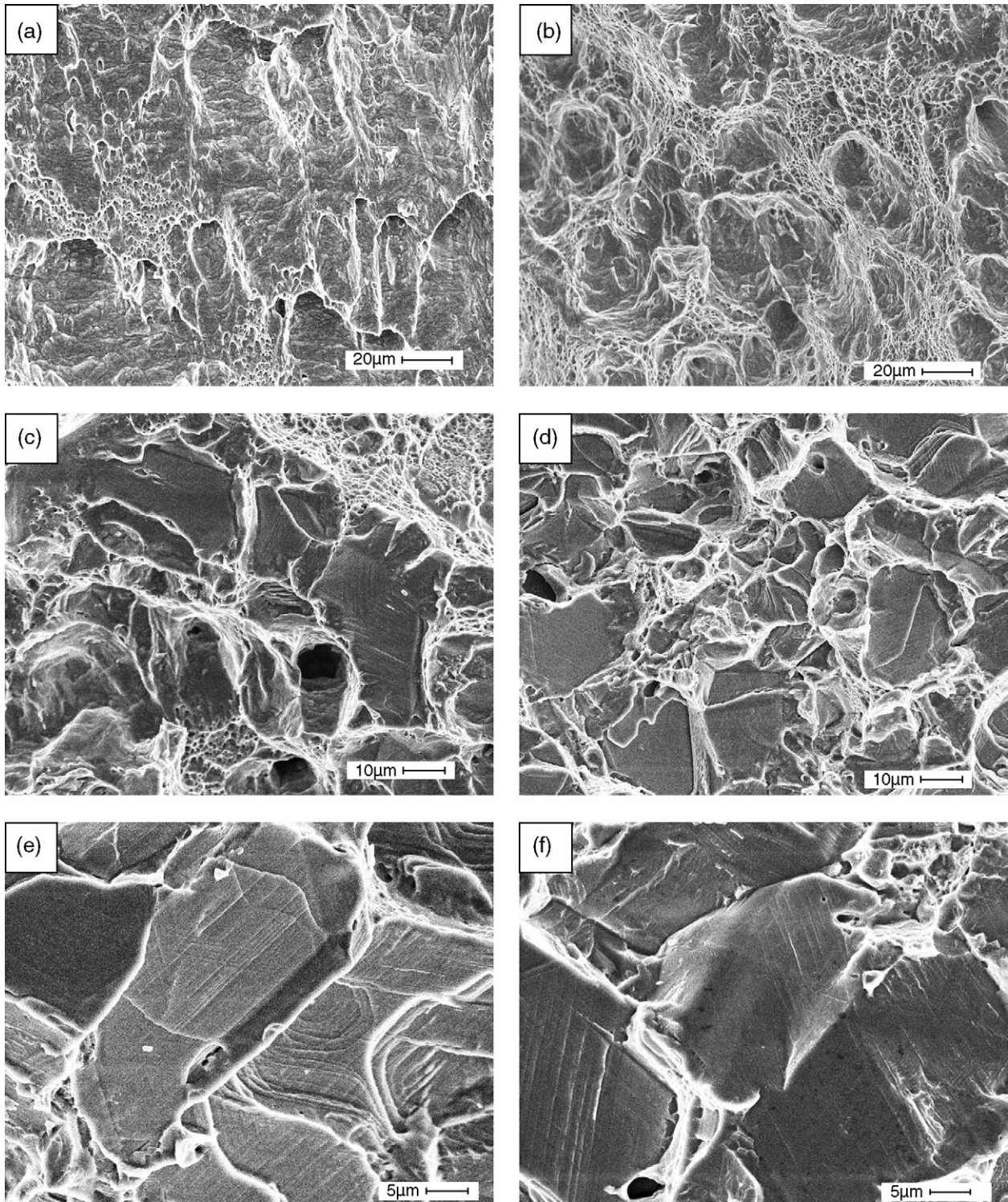


Fig. 2. Fractographs of 1# and 2#. (a, c, e) 1# impacted at 15,  $-100$  and  $-190$  °C, respectively and (b, d, f) 2# impacted at 15,  $-100$  and  $-190$  °C, respectively.

tents, both the 1# and 2# are still austenite even at liquid nitrogen temperature, which is confirmed by experiment and calculation [8,14]. It is well known that there are many slip systems in face-centered-cubic (fcc) austenite, as such, it will not occur cleavage fracture at most circumstances. But transgranular brittle fractures in nitrogen-alloyed austenitic stainless steel at low temperature are found by many researchers [2,3,10,11,18] and

also in this experiment. Whether ductile fracture or brittle fracture is decided by differences between shear resistance force  $\tau_K$  and direct resistance force  $S_{O\Gamma}$ . When  $\tau_K$  is higher than  $S_{O\Gamma}$ , the fracture is of brittle type. Generally,  $S_{O\Gamma}$  is independent of temperature, but  $\tau_K$  is of reverse relationship with temperature [19]. In HNASS, nitrogen will greatly increase slip resistance and interact with dislocation and stacking fault [20,21], which will

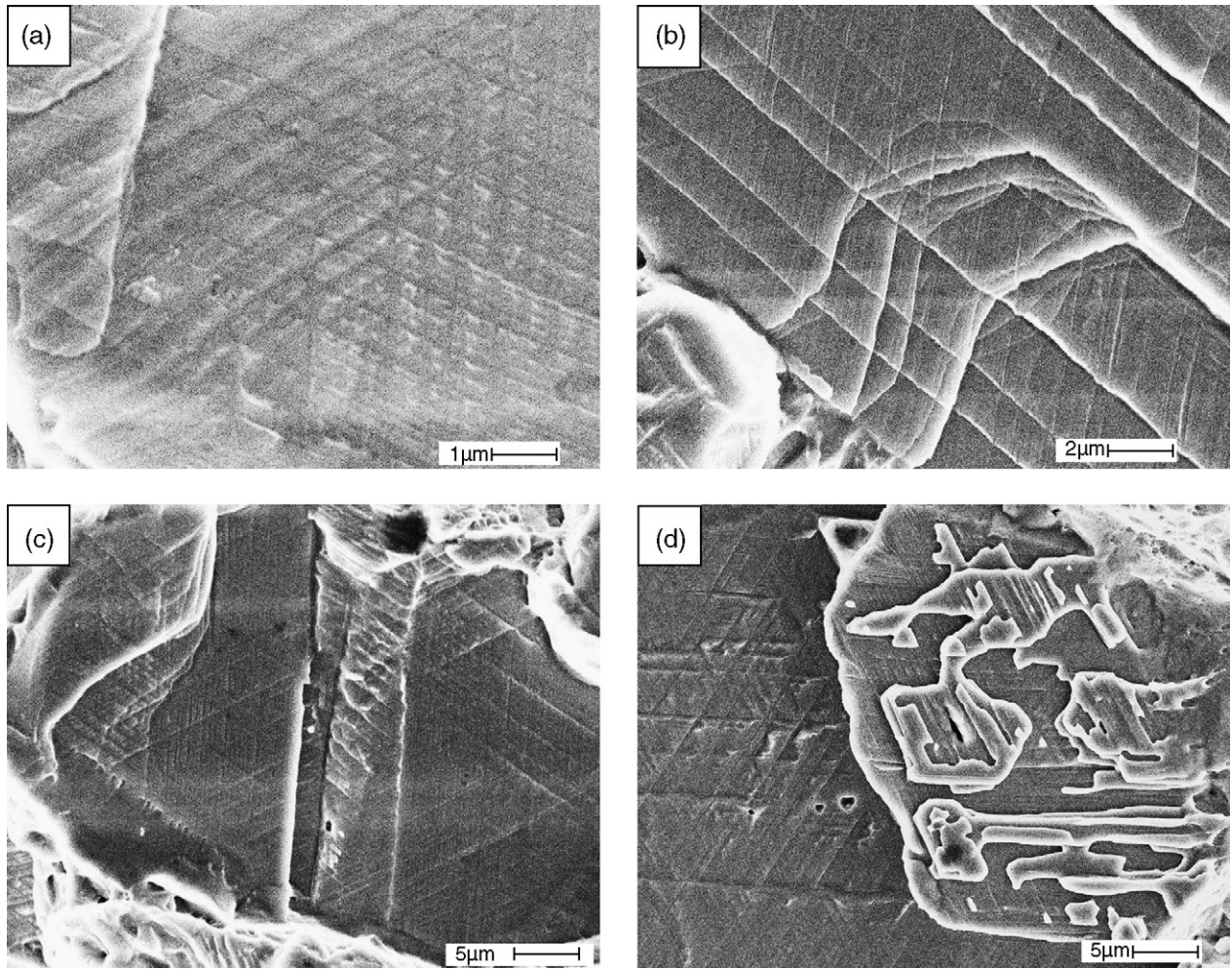


Fig. 3. Microstructures of (a) inter-crossed slip lines of 1# at  $-100^{\circ}\text{C}$ , (b) slip bands cross several (111) planes of 2# at  $-100^{\circ}\text{C}$ , (c) twinning gains of 2# at  $-190^{\circ}\text{C}$  and (d) peeled off layers of 1# at  $-190^{\circ}\text{C}$ .

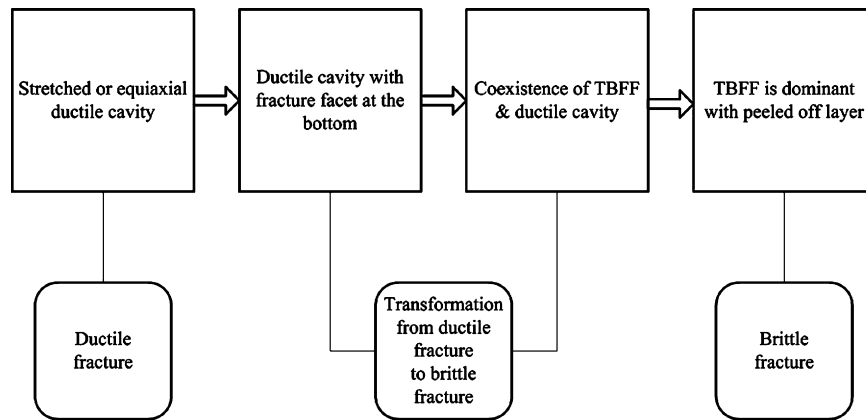


Fig. 4. Transformation of fracture microstructure with the descending temperatures.

become intense as temperature decreases and greatly increase the shear resistance force, when the temperature is low enough, the effect of nitrogen will be able to transform the fracture mode of HNASS materials from ductile fracture to brittle fracture. That is the reason for transgranular brittle fracture in fcc structures of HNASS at cryogenic temperature. So, peeled off layer is a good proof to  $\tau_K$  higher than  $S_{0\Gamma}$ .

#### 4. Conclusions

The impact properties of the two kinds of HNASSs become worse with the increase of nitrogen content. With the descending temperature, fracture pattern changes from ductile to brittle fracture. TBFF and peeled off layer are proves of brittle fracture in HNASS impacted at cryogenic temperature. All these effects

are mainly caused by high nitrogen content and its interactions with descending temperature.

### Acknowledgements

The authors would like to appreciate the support provided by the Materials Friction Key Laboratory, Natural Science Foundation of Jiangsu Province (No. KJS03006) and Specialized Research Fund for the Doctoral Program of Higher Education (SRFDP) (No. 20050299008).

### References

- [1] J.W. Simmons, *Mater. Sci. Eng. A* 207 (1996) 159–169.
- [2] Q. Dai, Y. Zheng, K. Chen, *Mater. Character.* 42 (1999) 21–26.
- [3] H. Hanninen, J. Romu, R. Ilola, J. Tervo, A. Laitinen, *J. Mater. Process. Technol.* 117 (2001) 424–430.
- [4] P. Fenici, D. Boerman, V. Coen, E. Lang, C. Ponti, W. Schule, *Nucl. Eng. Des.* 1 (1984) 167–183.
- [5] T. Kruml, J. Polak, S. Degallaix, *Mater. Sci. Eng. A* 293 (2000) 275–280.
- [6] Q. Dai, A. Wang, X. Cheng, L. Cheng, *Mater. Sci. Eng. A* 311 (2001) 205–210.
- [7] Z. Yuan, Q. Dai, X. Cheng, K. Chen, L. Pan, A. Wang, *Mater. Character.* 56 (2006) 79–83.
- [8] X. Cheng, Q. Dai, A. Wang, L. Cheng, *Mater. Sci. Eng. A* 311 (2001) 211–216.
- [9] A. Di Schino, J.M. Kenny, M.G. Mecozzi, M. Barteri, *J. Mater. Sci.* 35 (2000) 4803–4808.
- [10] R.L. Tobler, D. Meyn, *Metall. Mater. Trans. A* 19A (1988) 1626–1631.
- [11] Y. Tomota, J. Nakano, Y. Xia, K. Inoue, *Acta Mater.* 46 (1998) 3099–3108.
- [12] Q. Dai, Z. Yuan, X. Luo, X. Cheng, *Mater. Sci. Eng. A* 385 (2004) 445–448.
- [13] Q. Dai, X. Cheng, X. Luo, Y. Zhao, *Mater. Character.* 49 (2003) 367–371.
- [14] Q. Dai, X. Cheng, Y. Zhao, X. Luo, Z. Yuan, *Mater. Character.* 52 (2004) 349–354.
- [15] Q. Dai, S. Huo, *Chin. J. Mech. Eng.* 30 (1994) 14–18.
- [16] O. Yoo, Y.-J. Oh, B.-S. Lee, S.W. Nam, *Mater. Sci. Eng. A* 405 (2005) 147–157.
- [17] M.L. Saucedo-Munoz, Y. Watanabe, T. Shoji, H. Takahashi, *Cryogenics* 40 (2000) 693–700.
- [18] S. Liu, T. Hashida, H. Takahashi, H. Kuwano, Y. Hamaguchi, *Metall. Mater. Trans. A* 29 (1998) 791–798.
- [19] R. Yang, Q. Dai, *Mater. Character.* 38 (1997) 143–147.
- [20] P. Mullner, C. Solenthaler, P. Uggowitzzer, M.O. Speidel, *Mater. Sci. Eng. A* 164 (1993) 164–169.
- [21] P. Mullner, *Mater. Sci. Eng. A* 234–236 (1997) 94–97.